



High Expression of FAP in Colorectal Cancer Is Associated With Angiogenesis and Immunoregulation Processes

Mairene Coto-Llerena^{1†}, Caner Ercan^{1†}, Venkatesh Kancherla¹, Stephanie Taha-Mehlitz^{2,3}, Serenella Eppenberger-Castori¹, Savas D. Soysal³, Charlotte K. Y. Ng⁴, Martin Bolli³, Markus von Flüe³, Guillaume P. Nicolas⁵, Luigi M. Terracciano¹, Melpomeni Fani^{6*} and Salvatore Piscuoglio^{1,2,3*}

OPEN ACCESS

Edited by:

Fabio Iannelli,
IFOM - The FIRC Institute of Molecular
Oncology, Italy

Reviewed by:

Matteo Cereda,
Italian Institute for Genomic Medicine
(IIGM), Italy
Gianluca Matteoli,
KU Leuven, Belgium

*Correspondence:

Melpomeni Fani
Melpomeni.Fani@usb.ch
Salvatore Piscuoglio
Salvatore.Piscuoglio@usb.ch

†These authors have contributed
equally to this work

Specialty section:

This article was submitted to
Gastrointestinal Cancers,
a section of the journal
Frontiers in Oncology

Received: 10 February 2020

Accepted: 18 May 2020

Published: 08 July 2020

Citation:

Coto-Llerena M, Ercan C,
Kancherla V, Taha-Mehlitz S,
Eppenberger-Castori S, Soysal SD,
Ng CKY, Bolli M, von Flüe M,
Nicolas GP, Terracciano LM, Fani M
and Piscuoglio S (2020) High
Expression of FAP in Colorectal
Cancer Is Associated With
Angiogenesis and Immunoregulation
Processes. *Front. Oncol.* 10:979.
doi: 10.3389/fonc.2020.00979

¹Institute of Pathology and Medical Genetics, University Hospital Basel, Basel, Switzerland, ²Visceral Surgery Research Laboratory, Department of Biomedicine, University of Basel, Basel, Switzerland, ³Department of Visceral Surgery, Clarunis University Centre for Gastrointestinal and Liver Diseases, St. Clara Hospital and University Hospital Basel, Basel, Switzerland, ⁴Department for BioMedical Research (DBMR), University of Bern, Bern, Switzerland, ⁵Division of Nuclear Medicine, University Hospital Basel, Basel, Switzerland, ⁶Division of Radiopharmaceutical Chemistry, University Hospital Basel, University of Basel, Basel, Switzerland

Fibroblast activation protein α (FAP) plays an important role in tissue remodeling and helps tumor cells invade surrounding tissue. We sought to investigate FAP as a prognostic molecular marker in colorectal cancer (CRC) using immunohistochemical and transcriptomic data. FAP expression and clinicopathological information were obtained from The Cancer Genome Atlas data set. The association of FAP expression and tissue cellular heterogeneity landscape was explored using the xCell method. We evaluated FAP protein expression in a cohort of 92 CRCs and 19 non-tumoral tissues. We observed that FAP was upregulated in tumors both at the mRNA and protein levels, and its expression was associated with advanced stages, poor survival, and consensus molecular subtype 4. FAP expression was also associated with angiogenesis and collagen degradation. We observed an enrichment in immune-cell process-related genes associated with FAP overexpression. Colorectal cancers with high FAP expression display an inflamed phenotype enriched for macrophages and monocytes. Those tumors showed enrichment for regulatory T cell populations and depletion of T_H1 and natural killer T cells, pointing to an immunosuppressive environment. Colorectal cancers with high levels of stromal FAP are associated with aggressive disease progression and survival. Our results suggest that FAP plays additional roles in tumor progression such as modulation of angiogenesis and immunoregulation in the tumor microenvironment.

Keywords: colorectal cancer, cancer-associated fibroblast, immunohistochemistry, FAP, gene expression

INTRODUCTION

Tumor-infiltrating immune cells as well as cancer-associated fibroblasts (CAFs) are important components of the tumor microenvironment. In human cancer, the tumor microenvironment has been suggested as a new component for the classification of malignant tumors including colorectal cancers (CRCs) (1–3). In particular, CAFs play important roles in modulating tumor development

and prognosis via releasing proteolytic enzymes, growth factors, and immunomodulatory cytokines (4, 5).

Fibroblast activation protein α (FAP, also called seprase) is a prolyl-specific serine proteinase, highly upregulated in fibroblasts especially at sites of active tissue remodeling, including wound healing and fibrosis (6, 7). In CRC, previous studies reported the detection for FAP in more than 93% of the tumor. Among those, 30% showed high intensity for FAP staining (8). High FAP expression has been proposed as a biomarker for disease progression in metastatic CRCs (9). Similarly in rectal cancer, high FAP expression after preoperative chemoradiotherapy has been associated with poor prognosis (9). Given the scientific evidence, FAP has been considered as a candidate for targeted therapy in CRC. So far, diverse approaches, including FAP-targeting vaccines and immunotherapies, have been used in preclinical studies to deplete FAP-positive cells (10–12). Although these approaches have shown encouraging results in preclinical studies, those tested in clinical trials have shown limited efficacy, even in combination with chemotherapy (13–15). Furthermore, FAP-targeting radioligands have been used for *in vivo* imaging and targeted radionuclide therapy for a variety of cancers including CRC (16, 17).

Most of the functions described for FAP are associated with its enzymatic activity involved in tissue remodeling, which helps tumor cells invade the surrounding tissue, penetrate the blood vessel wall, and travel to form distant metastasis (18–21). Recent evidence suggested that FAP in CAFs could also play a critical role in regulating antitumor immune response by inducing tumor-promoting inflammation (22–24). This is particularly interesting because the majority of CRC patients are resistant to immunotherapies, especially to immune checkpoint blockades (25).

In our study, we sought to investigate FAP as a molecular marker in CRC using immunohistochemical and transcriptomic data. To investigate other potential roles of FAP in CRC, we explored its association with the clinicopathological characteristics of our in-house cohort. We further investigated its association at the mRNA level with molecular features, pathways and cell type populations in the tumor microenvironment using The Cancer Genome Atlas (TCGA) data set.

MATERIALS AND METHODS

Patients and Specimen Characteristics

One hundred primary unselected, non-consecutive CRCs treated at the University Hospital Basel between the years 2006 and 2012 were included in this study. A tissue microarray (TMA) of these 100 tumors was constructed. Briefly, tissue cylinders with a diameter of 1 mm were punched from morphologically representative areas of each donor block and brought into one recipient paraffin block (30 × 25 mm) using the TMA GrandMaster[®] (TMA-GM; 3D-Histech Ltd.; Sysmex AG, Horgen, Switzerland) technology. Each punch was derived from the center of the tumor in an area with no necrosis so that each TMA spot consisted of more than 50% tumor cells. For 30 cases, non-malignant adjacent mucosa was selected from

the same donor block. The study was performed in accordance with the Helsinki Declaration and approved by the ethics committee (Ethics Committee of Basel, EKBB, no. EKBB 361/12). Data were collected retrospectively in a non-stratified and non-matched manner including patient age, tumor diameter, location, pT/pN stage, grade, histologic subtype, vascular invasion, and clinical outcome. Intratumoral and peritumoral lymphocytic inflammation was evaluated using the original hematoxylin-eosin (H&E) slides of the resection specimens used as donor block. The tumor grade was categorized as low and high (≥ 50 , $< 50\%$ gland formation, respectively). The clinical outcome measure of interest was overall survival time.

Immunohistochemistry

Immunohistochemistry (IHC) was performed using an anti-FAP antibody (Vitatex, Stony Brook, NY, USA; seprase/FAP α ; dilution 1:100). Staining was performed on a Leica Bond III IHC staining system (Muttentz, Switzerland) using DAB as chromogen. Immunoreactivity was evaluated semiquantitatively as the proportion of positive staining in stromal cells in 10% increments, as well as the maximal staining intensity (0 = none, 1 = weak, 2 = intermediate, 3 = strong) by two experienced pathologists with expertise in gastrointestinal pathology (C.E. and L.M.T.). In terms of the percentage of FAP-positive cells, samples containing $< 10\%$ of positive cells were classified as low, whereas samples containing at least 10% of positive cells were classified as high as suggested by Henry et al. (8). In terms of FAP staining intensity, samples with intensities 0 or 1 were considered low, whereas samples with intensities 2 or 3 were considered high (8). In addition, 20 cases positive for FAP on TMA were reevaluated using whole sections from formalin-fixed paraffin-embedded tissue to study FAP expression heterogeneity. FAP immunostaining was evaluated both in stroma adjacent to the invasive tumor front and within the tumor center.

Tumor–Stromal Ratio

For all tumors, the tumor–stromal ratio on 4 μm H&E-stained tissue sections was calculated as described previously (26), and the stromal percentage was estimated per 10% intervals. Tumors were divided into stroma-high ($> 50\%$) and stroma-low ($\leq 50\%$) groups according to their highest score.

Assessment of Tumor Budding

Tumor budding was evaluated according to the International Tumor Budding Consensus Conference (ITBCC) method (27) and was defined according to ITBCC as single tumor cells or tumor cell clusters of up to four cells. Whole H&E-stained tissue sections of the tumors were used. One pathologist (C.E.) searched all tumor slides throughout at low magnification. Densest budding area at the invasive front (hot spot) was selected by visual estimation. Tumor buds in this area were counted at 20 \times magnification (field area, 0.785 mm²). Density of tumor buds was assigned into three grades: grade 1 (BD-1): 0–4 buds; grade 2 (BD-2): 5–9 buds; and grade 3 (BD-3): ≥ 10 buds.

Microsatellite Instability

Immunohistochemical analyses of mismatch repair proteins were performed for expression of the four mismatch repair proteins MLH1, MSH2, MSH6, and PMS2 as previously described (28). Tissue samples with tumor cells lacking nuclear staining for at least one of these proteins were considered to have a positive microsatellite instability (MSI) screening status, hereafter referred to as MSI. Negative MSI screening status based on immunohistochemical staining is hereafter referred to as microsatellite-stable.

Analysis of TCGA Data Set

FPKM gene-level expression data for TCGA colorectal carcinoma cohort (29) with 622 tumors and 51 non-tumoral tissues, defined as “solid tissue normal,” were obtained from TCGA Genomics Data Commons harmonized data portal using *TCGAbiolinks* R package (30). The expression of *FAP* was compared between tumors and normal tissues using the Student *t*-test. Tumor samples were classified into *FAP*-high and *FAP*-low groups based on the threshold of mean + 3 standard deviations of normal tissues. Clinical information was obtained from the Human Protein Atlas (Pathology Atlas) (31) CRC project for 596 TCGA CRCs.

Raw read counts of the TCGA CRC Project downloaded using *TCGAbiolinks* package (30) were used for differential expression analysis using the *edgeR* package (32). Genes with low expression (<1 log-counts per million in ≥ 50 samples) were filtered out. Normalization was performed using the “TMM” (weighted trimmed mean) method (33), and differential expression was assessed using the quasi-likelihood *F* test. Genes with log-fold change >2 and false discovery rate (FDR) <0.05 were considered differentially expressed. Pathway enrichment analysis of the upregulated genes from the differential analysis between the *FAP*-high and *FAP*-low groups was performed using clusterProfiler package (34), which supports Gene Ontology, KEGG, and Reactome Pathways. Significantly enriched pathways were selected based on FDR <0.05. Gene set enrichment analysis (GSEA) of all analyzed genes ranked based on signed *p* value according to the direction of the log-fold change was performed using the *fgsea* package (35). Gene Ontology gene sets from MSigDB (36) were used to identify significantly upregulated/downregulated pathways. Molecular subtyping was performed using *CMScaller* package (37), and the 622 TCGA CRCs were classified into 97 CMS1, 170 CMS2, 95 CMS3, 195 CMS4 subtypes, and 65 unclassified. Cell type enrichment analysis was performed with FPKM gene expression data using *xCell* gene signatures-based method for cell types (38).

Statistical Analysis

Statistical comparisons between categorical variables were performed using χ^2 test or Fisher exact test where appropriate. Statistical comparisons between numeric variables were performed using *t*-test, Mann–Whitney *U*-test, or paired Wilcoxon test. Survival analysis was performed using the Kaplan–Meier method and log-rank test. For the TCGA cohort, stratification of *FAP* expression for overall survival analysis was performed using the *maxstat* R package (39). Univariate Cox

regression analyses were performed to investigate the association between overall survival and clinical variables. Variables significant in univariate Cox regression analyses were included in multivariate Cox regression analysis. All tests were two-sided, and $p < 0.05$ was considered statistically significant. Statistical power of statistical tests was estimated by 100 iterations of bootstrapping. Statistical analysis was carried out with Prism (v7.0; San Diego, CA, USA) and R (v.3.6.1; R Foundation for Statistical Computing, Vienna, Austria. <http://www.R-project.org/>).

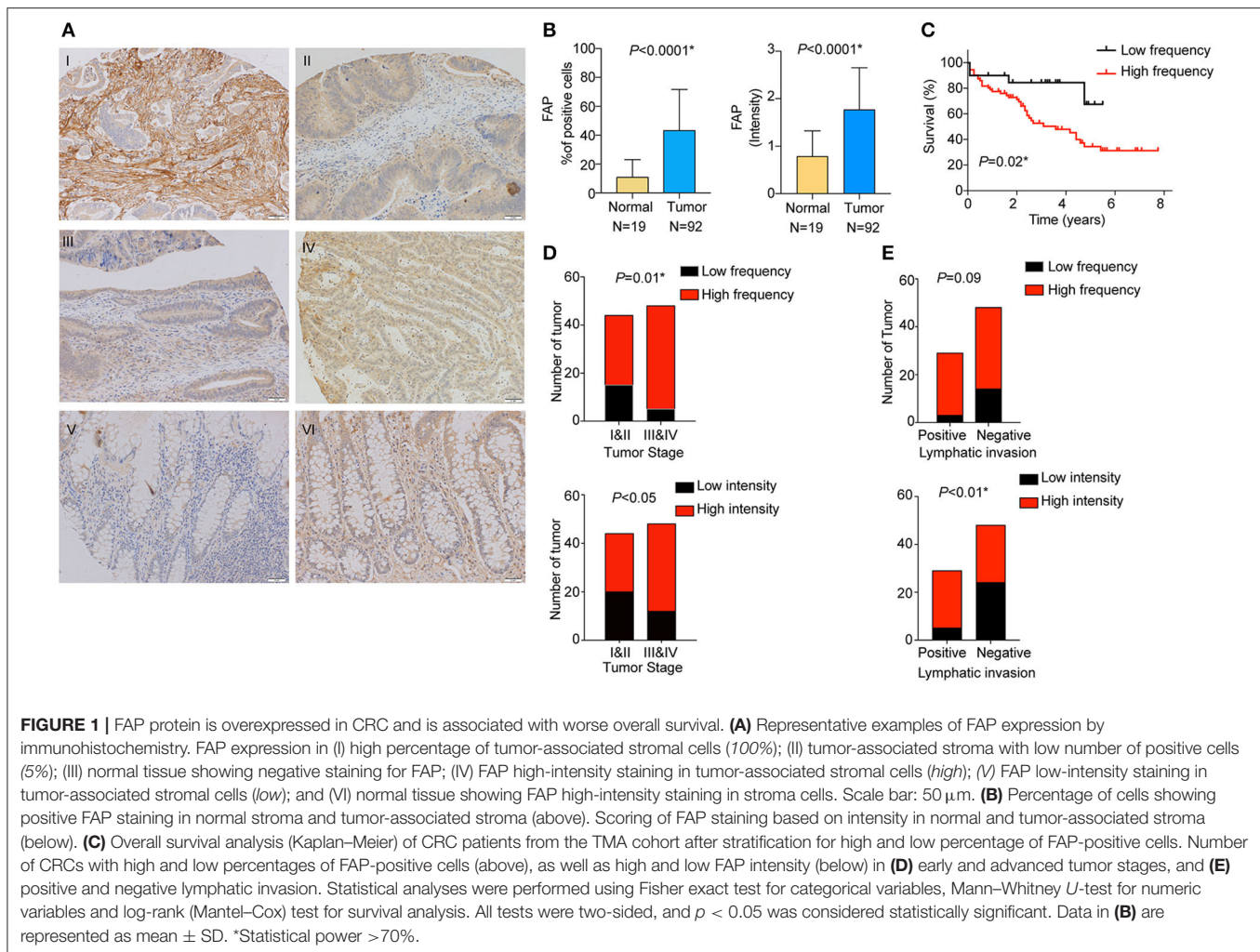
RESULTS

Expression of FAP in Colorectal Cancers

We analyzed the expression of *FAP* at the protein level in stromal cells by staining and scoring a TMA containing 100 CRC samples and 30 non-tumoral adjacent tissues using IHC (**Figure 1A**). After excluding samples for which the tissue core was absent or had poor staining quality, 92 CRCs and 19 non-tumoral colon samples were available for analysis. We observed a significantly higher percentage of *FAP*-positive stromal cells in tumors compared to non-tumoral tissues ($p < 0.0001$; **Figure 1B**). *FAP* expression was detected in 91% (84/92) of the tumors. High frequency (at least 10%) of *FAP*-positive cells was found in 78% (72/92) of CRCs, whereas high *FAP* intensity was observed in 66% (61/92, **Figure 1** and **Supplementary Figure 1A**). Sixty-three percent (58/92) had high frequency of *FAP*-positive cells with elevated intensity (2 or 3). Although *FAP* staining was detectable in 79% (15/19) of the non-tumoral tissue samples, both the number of positive cells and the intensity were significantly lower compared to tumoral tissue (both $p < 0.0001$; **Figure 1B**). Similar results were observed when we considered the 19 matched pairs of CRCs and non-tumoral colon samples ($p = 0.005$ for frequency and $p = 0.01$ for intensity; **Supplementary Figure 1B**). Of the 15 non-tumoral tissue samples with detectable *FAP* expression, only a single case showed a high percentage ($\geq 10\%$) of *FAP*-positive (intensity 2) cells.

We then investigated the association between *FAP* expression (both frequency and intensity) and the clinicopathological characteristics of our cohort (**Table 1**). We found that the frequency of *FAP*-positive cells and that of cells with high *FAP* intensity were significantly more frequently found in CRCs with advanced stages ($p = 0.01$ and $p < 0.05$, respectively, **Figure 1D**). Similarly, high *FAP* intensity was also associated with tumors showing high tumor grade and lymphovascular invasion ($p < 0.05$ and $p = 0.03$, respectively, **Table 1**). The lymphatic invasion was also associated with a high frequency of *FAP*-positive cells ($p = 0.09$, **Figure 1E** and **Table 1**) and a high *FAP* intensity ($p < 0.01$, **Figure 1E** and **Table 1**). We further observed a stepwise increase in tumor budding according to the percentage of *FAP*-positive cells ($p = 0.009$, **Supplementary Figure 1C**). No significant association was found with age, sex, tumor location, presence of MSI, stroma-to-tumor ratio, or venous invasion (**Table 1**).

Furthermore, we determined whether there was an association between the frequency of *FAP*-positive cells and overall survival. High frequency of *FAP*-positive cells, but not *FAP*



intensity, was associated with worse overall survival ($p = 0.02$; **Figure 1C** and **Supplementary Figure 1D**). Similarly, univariate and multivariate Cox regression analyses showed that FAP expression is an independent predictor of overall survival (**Supplementary Table 1**).

To cross-validate our results, we retrieved the gene expression data of 622 CRC cases from TCGA (29). In agreement with the data obtained by IHC on the TMA (**Figure 1B**), tumor samples expressed significantly higher levels of *FAP* compared to normal tissues ($p < 2.2 \times 10^{-16}$; **Figure 2A**). Association of *FAP* expression with clinicopathological parameters demonstrated that *FAP* overexpression was associated with more advanced tumor stage ($p = 0.02$, **Table 2** and **Figure 2C**). In terms of outcome, we observed a trend toward worse overall survival in patients with tumors with high *FAP* expression ($p = 0.06$; **Figure 2B** and **Supplementary Figure 2**). Univariate analysis found tumor stages and tumor location as predictors of overall survival, whereas *FAP* expression showed a trend to it ($p = 0.06$; **Supplementary Table 2**).

Taken together, our results suggest that FAP expression may be prognostic in CRC.

Transcriptomic Analysis of *FAP* Expression in Colorectal Tumors

To further understand the possible role of *FAP* in CRC, we analyzed the transcriptomic data from the TCGA data set ($n = 622$). We investigated the association of *FAP* expression with the CRC molecular subtypes, and we observed a statistically significant association with tumors classified as CMS1 and CMS4 ($p = 0.02$ and $p < 0.001$; **Figure 3A** and **Table 2**). CMS1 and CMS4 have been reported to be associated with an upregulation of immune response genes and epithelial-to-mesenchymal transition, respectively (40). In particular, the association with CMS4 suggests a more aggressive origin of these tumors characterized by *FAP* overexpression.

Then, we performed a differential expression analysis between CRCs with high vs. low *FAP* expression. The differential expression analysis revealed 655 up- and 9 downregulated genes. Consistent with previous reports (41, 42), we found that the upregulated genes were enriched in functions related to collagen degradation, extracellular organization, regulation of cell-to-cell adhesion,

TABLE 1 | Association between FAP protein expression and clinicopathological features in the TMA cohort.

| Clinical features | Frequency | | | Intensity | | |
|------------------------------------|---------------------|--------------------|----------|---------------------|--------------------|----------|
| | High FAP expression | Low FAP expression | <i>p</i> | High FAP expression | Low FAP expression | <i>p</i> |
| Age (years) | | | | | | |
| <59 | 9 (82%) | 2 (18%) | 0.64 | 7 (64%) | 4 (36%) | 0.11 |
| 60–69 | 16 (73%) | 6 (27%) | | 11 (50%) | 11 (50%) | |
| 70–79 | 24 (86%) | 4 (14%) | | 23 (82%) | 5 (18%) | |
| >80 | 23 (74%) | 8 (26%) | | 19 (61%) | 12 (39%) | |
| Sex | | | | | | |
| Male | 42 (78%) | 12 (22%) | 1 | 34 (63%) | 20 (37%) | 0.66 |
| Female | 30 (79%) | 8 (21%) | | 26 (68%) | 12 (32%) | |
| Tumor location | | | | | | |
| Cecum | 14 (82%) | 3 (18%) | 0.96 | 13 (76%) | 4 (24%) | 0.73 |
| Ascending colon | 12 (80%) | 3 (20%) | | 8 (53%) | 7 (47%) | |
| Transverse colon | 4 (80%) | 1 (20%) | | 4 (80%) | 1 (20%) | |
| Descending colon | 6 (67%) | 3 (33%) | | 5 (56%) | 4 (44%) | |
| Sigmoid colon | 20 (77%) | 6 (23%) | | 16 (62%) | 10 (38%) | |
| Rectum | 16 (80%) | 4 (20%) | | 13 (65%) | 7 (35%) | |
| Stage | | | | | | |
| I | 10 (59%) | 7 (41%) | 0.03 | 11 (65%) | 6 (35%) | 0.14 |
| II | 19 (70%) | 8 (30%) | | 13 (48%) | 14 (52%) | |
| III | 25 (93%) | 2 (7%) | | 20 (74%) | 7 (26%) | |
| IV | 18 (86%) | 3 (14%) | | 16 (76%) | 5 (24%) | |
| Grade | | | | | | |
| Low | 51 (75%) | 17 (25%) | 0.26 | 40 (59%) | 28 (41%) | <0.05 |
| High | 21 (88%) | 3 (12%) | | 20 (83%) | 4 (17%) | |
| Tumor: stroma* | | | | | | |
| Stroma low | 55 (77%) | 16 (23%) | 1 | 46 (65%) | 25 (35%) | 1 |
| Stroma high | 17 (68%) | 4 (32%) | | 14 (66%) | 7 (34%) | |
| Microsatellite instability* | | | | | | |
| MSI | 9 (90%) | 1 (10%) | 0.45 | 9 (90%) | 1 (10%) | 0.09 |
| MSS | 62 (77%) | 19 (23%) | | 50 (62%) | 31 (38%) | |
| Lymphatic invasion | | | | | | |
| Positive | 26 (90%) | 3 (10%) | 0.09 | 24 (83%) | 5 (17%) | <0.01** |
| Negative | 34 (71%) | 14 (29%) | | 24 (50%) | 24 (50%) | |
| Venous invasion* | | | | | | |
| Positive | 16 (76%) | 5 (24%) | 1 | 13 (61%) | 8 (38%) | 1 |
| Negative | 44 (76%) | 14 (24%) | | 35 (60%) | 23 (40%) | |
| Lymphovascular invasion* | | | | | | |
| Positive | 32 (84%) | 6 (16%) | 0.2 | 29 (76%) | 9 (24%) | 0.03 |
| Negative | 33 (72%) | 13 (28%) | | 24 (52%) | 22 (48%) | |

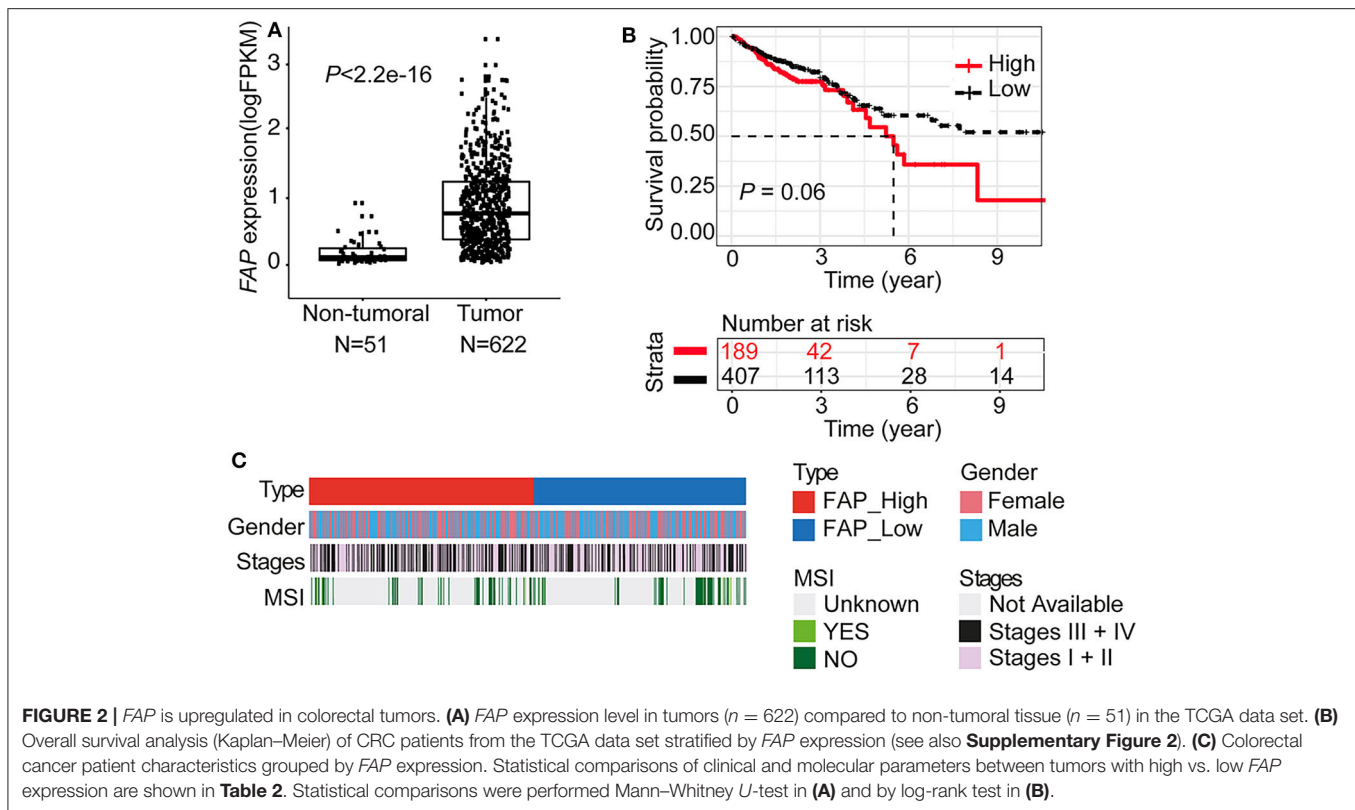
All 2 × 2 contingency tables were analyzed with Fisher exact tests. All others by χ^2 test.

*Patients with data not available, unknown, and discrepancies.

**Statistical power estimated by bootstrapping.

and cell junction organization (**Figure 3B**). Additionally, pathways involved in epithelial cell proliferation, invasion, and immune surveillance such as regulation of Wnt signaling, ERK1, and ERK2 cascade and angiogenesis

were also associated with *FAP* upregulation (**Figure 3B**). We further performed a GSEA by ranking all expressed genes based on the signed *p*-value from the differential expression analysis according to the direction of the log-fold



change (**Supplementary Figure 3**). We observed that *FAP* overexpression was associated with processes related to epithelial-to-mesenchymal transition, angiogenesis, tissue remodeling, epithelial cell proliferation, and immune response (**Supplementary Figures 3, 4**).

Because we observed that *FAP* overexpression was associated with immune-related processes (**Figure 3C** and **Supplementary Figure 3**), we sought to explore which immune components may be involved. We observed that CRCs with high *FAP* expression showed high expression of genes such as *FOXP3*, *CTLA4*, *ICOS*, and *KLRG1* (**Figure 3C**), which are usually expressed in immune cell populations such as regulatory T cells (Tregs) or in populations showing an immunosuppressive phenotype. To evaluate whether *FAP* overexpression was associated with the enrichment of specific immune cell populations, we used xCell, a method to perform cell type enrichment analysis from gene expression data for 64 immune and stromal cell types, on the TCGA CRC cohort. Overall, we found that tumors with high *FAP* expression were enriched for both immune and stromal cell types compared to tumors with low *FAP* expression (**Figure 3D** and **Supplementary Figure 5**). Populations such as endothelial cells and fibroblasts were found to be more abundant in *FAP*-overexpressing CRC ($p = 3.1e-13$ and $p = 6.9e-11$, respectively; **Figures 3D,E**). Similarly, macrophages, monocytes, and Tregs were also enriched in *FAP*-overexpressing samples. Interestingly, *FAP*-overexpressing CRCs were depleted for populations associated with antitumoral responses such as

T_H1 cells and natural killer T (NKT) cells. No significant differences were found regarding CD8T cells, T_H2 cells, or B cells.

Taken together, our results suggest that *FAP* may contribute to the poor prognosis of CRC by modulating the tumor microenvironment not only by driving angiogenesis but also by promoting a more protumorigenic environment.

FAP Distribution in the Tumor Center and Invasive Tumor Front

Given that the transcriptomic analysis suggests that *FAP* may promote a protumorigenic environment, we investigated whether the localization of *FAP* in the tumor could be associated with its role in CRC invasion. We took advantage of 20 CRCs that showed positive *FAP* staining in the TMA and stained whole tissue sections to define *FAP* heterogeneity. Using whole sections, we were able to visualize the tumor center and the invasive front in 95% (19/20) of the samples. *FAP* staining was visible in both tumor center and tumor front in all 19 cases (**Figure 4A**). Compared to the tumor center, *FAP*-positive cells were more frequently found at the invasive front ($p = 0.03$; **Figure 4B**). The high frequency of *FAP*-positive cells at the invasive front was associated with advanced tumor stage ($p = 0.03$; **Figure 4C**; right), but no significant association was found between the frequency of *FAP*-positive cells in the tumor center and tumor stage (**Figure 4C**; left). The presence of lymphovascular invasion was significantly associated with high

TABLE 2 | Association between *FAP* mRNA expression and clinicopathological features in the TCGA cohort.

| Clinical features | | Low <i>FAP</i> expression | High <i>FAP</i> expression | <i>p</i> |
|---|--|---------------------------|----------------------------|----------|
| | | n (%) | n (%) | |
| Gender (<i>n</i> = 591) | Female (<i>n</i> = 271) | 133 (49.1%) | 138 (50.9%) | 0.81 |
| | Male (<i>n</i> = 320) | 154 (48.1%) | 166 (51.9%) | |
| AJCC stages (<i>n</i> = 571)* | Stage I + II (<i>n</i> = 316) | 167 (52.8%) | 149 (47.2%) | 0.02 |
| | Stage III + IV (<i>n</i> = 255) | 111 (43.5%) | 144 (56.5%) | |
| Microsatellite instability (<i>n</i> = 115)* | MSI (<i>n</i> = 11) | 7 (63.6%) | 4 (36.4%) | 0.42 |
| | MSS (<i>n</i> = 104) | 53 (51.0%) | 51 (49.0%) | |
| CRC subtyping (<i>n</i> = 556)* | CMS1 (<i>n</i> = 97) | 36 (37.1%) | 61 (62.9%) | <0.001** |
| | CMS2 (<i>n</i> = 170) | 129 (75.9%) | 41 (24.1%) | |
| | CMS3 (<i>n</i> = 94) | 66 (70.2%) | 28 (29.8%) | |
| | CMS4 (<i>n</i> = 195) | 17 (8.7%) | 178 (91.3%) | |
| CRC location (<i>n</i> = 597)* | Cecum (<i>n</i> = 106) | 56 (52.8%) | 50 (47.2%) | 0.4 |
| | Ascending colon (<i>n</i> = 86) | 31 (36.0%) | 55 (64.0%) | |
| | Descending colon (<i>n</i> = 20) | 9 (45.0%) | 11 (55.0%) | |
| | Transverse colon (<i>n</i> = 38) | 20 (52.6%) | 18 (47.4%) | |
| | Sigmoid colon (<i>n</i> = 155) | 75 (48.4%) | 80 (51.6%) | |
| | Hepatic flexure (<i>n</i> = 26) | 12 (46.2%) | 14 (53.8%) | |
| | Splenic flexure (<i>n</i> = 7) | 4 (57.0%) | 3 (43.0%) | |
| | Rectosigmoid junction (<i>n</i> = 49) | 24 (49.0%) | 25 (51.0%) | |
| | Rectum (<i>n</i> = 110) | 60 (55.0%) | 50 (45.0%) | |

*Patients with data not available, unknown, and discrepancies.

**Statistical power >70% (estimated by bootstrapping).

All 2 × 2 contingency tables were analyzed with Fisher exact tests. All others by χ^2 test.

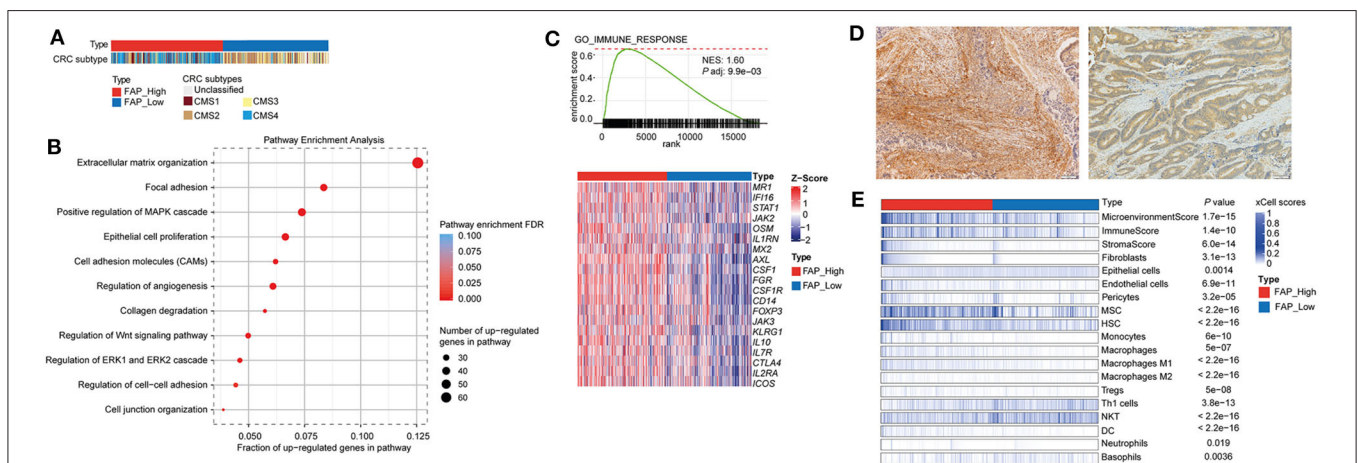
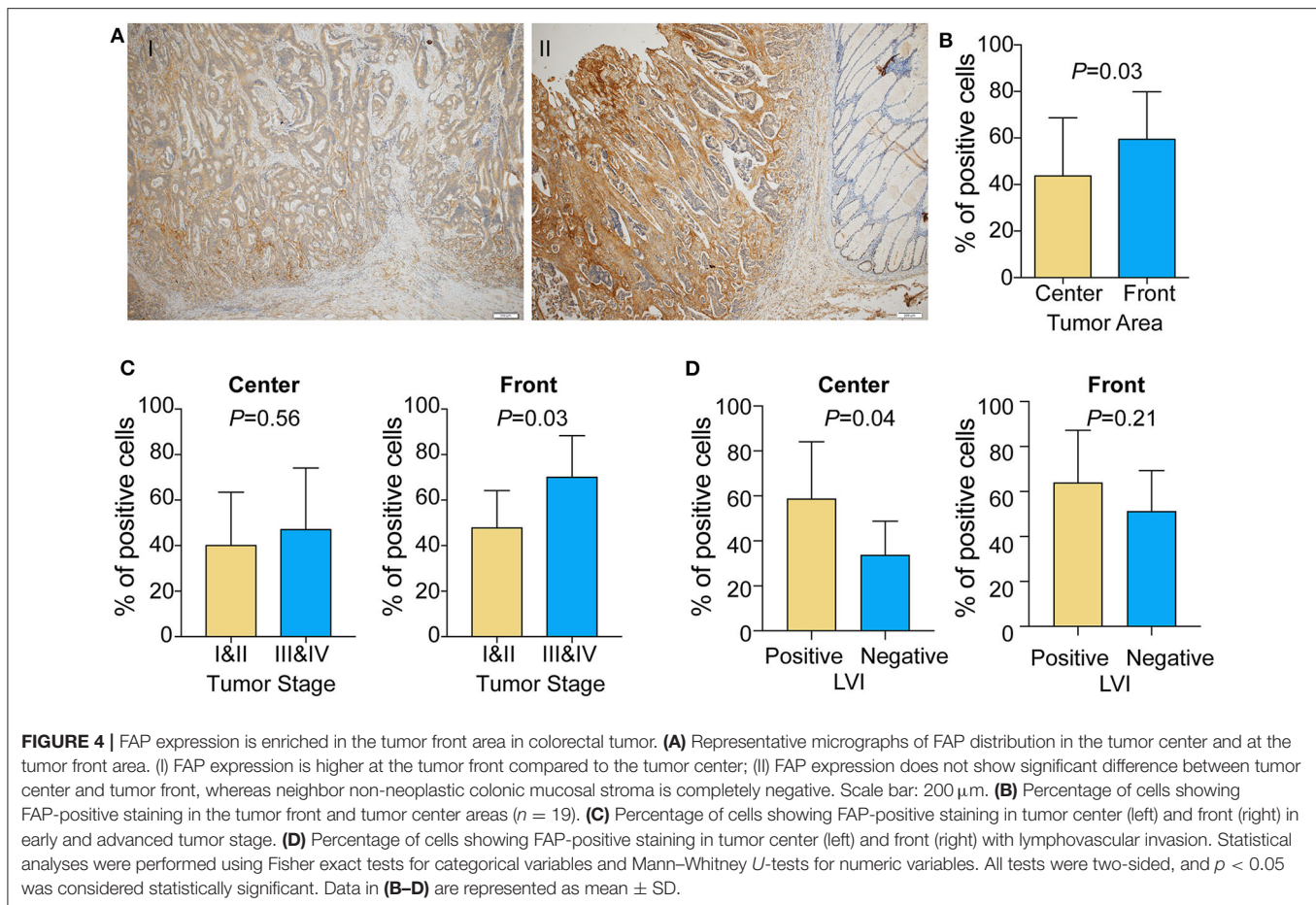


FIGURE 3 | *FAP* is associated with pathways involved in tumor growth, invasion, and immunosuppressive tumor microenvironment. **(A)** Colorectal cancers grouped by *FAP* expression. Statistical comparison of molecular subtypes between tumors with high vs. low *FAP* expression are shown in **Table 2**. **(B)** Figure shows selected significantly enriched pathways from pathway enrichment analysis of the upregulated genes from a differential expression analysis between *FAP*-high vs. *FAP*-low. The size of the dots indicates the number of upregulated genes in each pathway. The color of the dot indicates FDR, and x axis represents the fraction of upregulated genes in the pathway. **(C)** Gene set enrichment analysis plots of GO immune response, where x axis shows ranked list of genes (ranked by the *p*-values signed according to the direction of the differential expression analysis between *FAP*-high and *FAP*-low CRCs), and the vertical bars below the x axis show the genes that belong to gene set. The y axis shows the enrichment score of the gene set. Heatmaps below show selected genes in the GO process. **(D)** Representative pictures showing the enrichment of fibroblast on high *FAP* expression (left) and low number of fibroblasts on low *FAP* expression (right). **(E)** Heatmap shows the enrichment of immune and stromal cell types in the TCGA CRC cohort, as defined by the xCell method. Samples were stratified into *FAP*-high and *FAP*-low groups and then sorted based on their xCell fibroblasts scores. Cell types that showed statistically significant difference between *FAP*-high and *FAP*-low groups are shown. Statistical comparisons were performed using Mann-Whitney *U*-tests.



frequency of FAP-positive cells in tumor center (**Figure 4D**, $p = 0.04$) but not in tumor front.

These results are in line with the results we obtained by TMA, underlying the important role of FAP in tumor invasion.

DISCUSSION

FAP has been shown to be overexpressed in tumor-associated stromal cells in epithelial tumors (43) and its presence has been associated with worse prognosis. Moreover, tumors showing upregulation of FAP present a high level of microvessel density (44), which is also a marker for poor prognosis in several epithelial cancers (45–47). *In vivo* studies have shown that FAP overexpression in breast and colonic xenograft models leads to more rapid development of subcutaneous tumors and enhanced tumor growth (44). By contrast, inhibition of FAP activity in colorectal xenograft models results in tumor growth attenuation (48). Together, there is substantial evidence supporting the role of FAP in tumor proliferation and metastasis (49). Moreover, little is known about the molecular role of FAP in CRC and its potential in modulating the tumor microenvironment. This is particularly important because immune checkpoint inhibitors have demonstrated little or no clinical activity in the majority of patients with metastatic CRC (50).

In the present study, we investigated the expression of FAP both at the RNA and protein levels in two independent cohorts of CRC and its association with clinicopathological features. Similarly to previous reports evaluating FAP expression using IHC (8, 9, 51, 52), FAP was found upregulated in tumors compared to non-tumoral tissues and was associated with poor survival in both cohorts. In line with the poor prognosis, we found that high frequency of FAP-positive cells and high FAP intensity at the protein and RNA levels were associated with advanced stages. Although our results are discrepant from previous works showing FAP expression was also elevated in early-stage CRC (8, 51), we also found that FAP expression was associated with lymphatic invasion and tumor budding. Lymphatic invasion has been used to estimate the aggressiveness of colorectal tumors (53), whereas tumor budding is a surrogate for epithelial-to-mesenchymal transition and is associated with poor prognosis (54). The findings related to pathological features are thus in agreement with the association with advanced stages. Taken together, the association of FAP expression on the mRNA and protein levels with multiple clinicopathological features known to be associated with poor prognosis supports our finding that FAP is also associated with tumor aggressiveness.

Most studies on FAP have focused on its potential value as a prognostic marker in epithelial cancers, but little is known on

how and why FAP may be prognostic. We, therefore, analyzed the transcriptomic data from 622 CRCs in the TCGA. We found that the majority of tumors with high FAP expression were classified as CMS1 and CMS4 of the consensus molecular subtypes. CMS4 tumors have been reported to overexpress proteins implicated in stromal invasion, mesenchymal activation, and complement pathways. The enrichment for CMS4 tumors among tumors with high FAP expression suggests a more invasive tumor phenotype, which agrees with our findings from the TMA. In fact, our analysis of the TCGA transcriptomic data also showed that CRCs with FAP overexpression were enriched for stromal cell types, in particular for fibroblasts and mesenchymal stem cells. Furthermore, most of the pathways associated with FAP overexpression were related to extracellular matrix, junction remodeling, and collagen degradation, all of which have previously been associated with FAP expression. We further found that epithelial-to-mesenchymal transition, angiogenesis, and epithelial cell proliferation were also enriched in FAP-overexpressing CRCs. Our results are in line with previous studies that have demonstrated the involvement of FAP in epithelial-to-mesenchymal transition, angiogenesis, and in tumorigenesis (44, 49, 55). Additionally, our IHC analysis showed that the frequency of FAP-positive cells was associated with tumor budding score, a very well-known pathological marker associated with epithelial-to-mesenchymal transition and tumor invasion. Overall, the findings from our analysis of the TCGA are further supported by the observation that FAP was preferentially found at the tumor invasive front, in agreement with Sandberg et al. (56), suggesting a role in tissue invasion and metastasis.

In addition to CMS4, we also found that FAP-overexpressing CRCs were enriched in the subtype CMS1. While the most widely described function of FAP on CAFs in CRC was extracellular matrix remodeling (57), new evidence suggests that FAP on CAFs also has critical roles in regulating antitumor immune response by inducing tumor-promoting inflammation (58). Indeed, the CMS1 subtype displays upregulation of proteins involved in immune response pathways (40). We also found that FAP overexpression is associated with an upregulation of genes involved in immune cell response, suggesting that FAP may promote an inflamed environment. Recent reports have proposed that FAP expression may be associated with resistance to immune therapies (22, 59). Using the xCell algorithm, we found that populations such as T_H1 and NKT cells were suppressed, whereas Tregs were enriched in FAP-overexpressing CRCs, suggesting an immunosuppressive environment in these tumors. Chen et al. (23) reported that FAP expression promotes immunosuppression in a CRC tumor model via the upregulation of CCL2. CCL2, a member of the C-C chemokine family, regulates the recruitment of myeloid cells, mostly macrophages and monocytes (60), into inflamed sites to promote tumor growth (61, 62). In breast cancer, Costa et al. (63) showed that CAF with high expression of FAP was associated with increased CD25⁺FOXP3⁺ T lymphocytes via the modulation of B7H3, DPP4, and CD73. Accordingly, we also observed that macrophage and monocyte populations are enriched in FAP-overexpressing CRCs.

Although the statistical power of our study is limited by the relatively small sample size of the TMA cohort, our study is still one of the largest cohorts evaluating FAP expression in CRCs. Our results support the well-known role of FAP in promoting tumor growth and invasion. Based on our results, we speculate that one of the mechanisms by which FAP promotes tumorigenesis is linked to its ability to recruit endothelial cells and to induce angiogenesis, together with its enzymatic activity. Moreover, FAP will orchestrate a broad panel of other cells to push microenvironment toward an immunosuppressive environment, thus providing a niche for a more aggressive CRC phenotype.

DATA AVAILABILITY STATEMENT

Publicly available datasets were analyzed in this study. This data can be found here: TCGA data portal (<https://portal.gdc.cancer.gov/>).

ETHICS STATEMENT

The studies involving human participants were reviewed and approved by Ethics Committee of Basel, EKBB, number EKBB 361/12. The patients/participants provided their written informed consent to participate in this study.

AUTHOR CONTRIBUTIONS

MC-L, LT, MF, and SP: conceived the study. MC-L and SP: supervised the study. VK: performed bioinformatic analysis. CE and LT: performed the histologic review and immunohistochemical evaluation. MC-L, CE, ST-M, and SP: analyzed the results. SS, MB, MvF, GN, and MF: carefully discussed the results. MC-L, CE, and VK: wrote the manuscript that was revised by CN and SP. All authors edited and approved the final draft of the manuscript and are accountable for all aspects of the work.

FUNDING

Financial support was provided by the Swiss National Science Foundation [Ambizione PZ00P3_168165 to SP]. The funding body had no role in study design; in the collection, analysis and interpretation of data; in the writing of the report; and in the decision to submit the article for publication.

ACKNOWLEDGMENTS

We thank the tissue biobank of the Institute of Pathology at the University Hospital of Basel for providing slides of the TMA. Part of this study has been presented as poster at Swiss Society of Pathology conference and the European Congress of Pathology in 2019.

SUPPLEMENTARY MATERIAL

The Supplementary Material for this article can be found online at: <https://www.frontiersin.org/articles/10.3389/fonc.2020.00979/full#supplementary-material>

Supplementary Figure 1 | (A) Table displays the distribution of frequency of FAP-positive cells and FAP intensity in the TMA cohort. (B) Frequency (left) and intensity (right) of FAP-positive cells in 19 non-malignant tissues and paired malignant tissues. (C) Percentage of cells showing FAP-positive staining (left) or intensity (right) associated with tumor budding score. (D) Overall survival analysis (Kaplan–Meier) of CRC patients from the TMA cohort after stratification (below) for tumors with high FAP intensity vs tumors with low FAP intensity and (above) for tumors with high frequency of FAP-positive cells and/or high FAP intensity vs tumors with low frequency of FAP-positive cells and low FAP intensity. Data in (B,C) are represented as mean \pm SD. Statistical analyses were performed using Fisher exact tests for categorical variables in (B), ANOVA in (C) and log-rank (Mantel–Cox) tests for survival analysis in (D). All tests were two-sided, and $p < 0.05$ was considered statistically significant. *Statistical power $>70\%$.

Supplementary Figure 2 | The plot shows the optimal cutpoint for the stratification of TCGA CRC cohort into two groups, FAP-high and FAP-low, for overall survival analysis.

Supplementary Figure 3 | (A) Gene Set Enrichment Analysis plot shows selected significantly enriched Gene Ontology gene sets from MSigDB database

in FAP-high tumors in the TCGA CRC cohort. (B) Gene Set Enrichment Analysis plots of Gene Ontology molecular functions, where x-axis shows ranked list of genes (ranked by the p -values signed according to the direction of the differential expression analysis between FAP-high and FAP-low CRCs) and the vertical bars on the x-axis show the genes that belong to gene set. The y-axis shows the enrichment score of the gene set. Heatmaps below show selected genes in each GO process. Pearson correlation coefficients of the expression of the genes with FAP expression are shown to the right. NES: normalized enrichment score. P adj, p -value adjusted for multiple testing (i.e., FDR).

Supplementary Figure 4 | Correlation of FAP expression with (A) immune markers; (B) epithelial to mesenchymal transition (EMT) markers and (C) angiogenesis markers. Statistical analyses were performed using Pearson correlation tests.

Supplementary Figure 5 | Boxplots show the enrichment scores of each cell type between FAP-high and FAP-low groups in the TCGA CRC cohort, as defined by xCell. p -values were calculated using t-tests.

Supplementary Table 1 | Univariate and multivariate Cox regression analyses for the effect of FAP protein expression and clinicopathological parameters on overall survival in the TMA cohort.

Supplementary Table 2 | Univariate and multivariate Cox regression analyses for the effect of FAP mRNA expression and clinicopathological parameters on overall survival in the TCGA cohort.

REFERENCES

- Galon J, Mlecnik B, Bindea G, Angell HK, Berger A, Lagorce C, et al. Towards the introduction of the “Immunoscore” in the classification of malignant tumours. *J Pathol.* (2014) 232:199–209. doi: 10.1002/path.4287
- Park JH, Richards CH, McMillan DC, Horgan PG, Roxburgh CSD. The relationship between tumour stroma percentage, the tumour microenvironment and survival in patients with primary operable colorectal cancer. *Ann Oncol.* (2014) 25:644–51. doi: 10.1093/annonc/mdt593
- Eriksen AC, Sørensen FB, Lindebjerg J, Hager H, Christensen RD, Kjær-Frifeldt S, et al. The prognostic value of tumour stroma ratio and tumour budding in stage II colon cancer. A nationwide population-based study *Int J Colorectal Dis.* (2018) 33:1115–24. doi: 10.1007/s00384-018-3076-9
- Kuzet S-E, Gaggioli C. Fibroblast activation in cancer: when seed fertilizes soil. *Cell Tissue Res.* (2016) 365:607–19. doi: 10.1007/s00441-016-2467-x
- Koliaraki V, Pallangyo CK, Greten FR, Kollias G. Mesenchymal cells in colon cancer. *Gastroenterology.* (2017) 152:964–79. doi: 10.1053/j.gastro.2016.11.049
- Niedermeyer J, Garin-Chesa P, Kriz M, Hilberg F, Mueller E, Bamberger U, et al. Expression of the fibroblast activation protein during mouse embryo development. *Int J Dev Biol.* (2001) 45:445–7.
- Jacob M, Chang L, Pure E. Fibroblast activation protein in remodeling tissues. *Curr Mol Med.* (2012) 12:1220–43. doi: 10.2174/156652412803833607
- Henry LR, Lee H-O, Lee JS, Klein-Szanto A, Watts P, Ross EA, et al. Clinical implications of fibroblast activation protein in patients with colon cancer. *Clin Cancer Res.* (2007) 13:1736–41. doi: 10.1158/1078-0432.CCR-06-1746
- Saigusa S, Toiyama Y, Tanaka K, Yokoe T, Okugawa Y, Fujikawa H, et al. Cancer-associated fibroblasts correlate with poor prognosis in rectal cancer after chemoradiotherapy. *Int J Oncol.* (2011) 38:655–63. doi: 10.3892/ijo.2011.906
- Lee J, Fassnacht M, Nair S, Boczkowski D, Gilboa E. Tumor immunotherapy targeting fibroblast activation protein, a product expressed in tumor-associated fibroblasts. *Cancer Res.* (2005) 65:11156–63. doi: 10.1158/0008-5472.CAN-05-2805
- Ostermann E, Garin-Chesa P, Heider KH, Kalat M, Lamche H, Puri C, et al. Effective immunoconjugate therapy in cancer models targeting a serine protease of tumor fibroblasts. *Clin Cancer Res.* (2008) 14:4584–92. doi: 10.1158/1078-0432.CCR-07-5211
- Loeffler M, Krüger JA, Niethammer AG, Reisfeld RA. Targeting tumor-associated fibroblasts improves cancer chemotherapy by increasing intratumoral drug uptake. *J Clin Investig.* (2009) 119:421. doi: 10.1172/JCI26532C1
- Narra K, Mullins SR, Lee H-O, Strzemkowski-Brun B, Magalano K, Christiansen VJ, et al. Phase II trial of single agent Val-boroPro (talabostat) inhibiting fibroblast activation protein in patients with metastatic colorectal cancer. *Cancer Biol Therap.* (2007) 6:1691–9. doi: 10.4161/cbt.6.1.14874
- Eager RM, Casey Cunningham C, Senzer NN, Stephenson J, Anthony SP, O’Day SJ, et al. Phase II assessment of talabostat and cisplatin in second-line stage IV melanoma. *BMC Cancer.* (2009) 9:263. doi: 10.1186/1471-2407-9-263
- Eager RM, Cunningham CC, Senzer N, Richards DA, Raju RN, Jones B, et al. Phase II trial of talabostat and docetaxel in advanced non-small cell lung cancer. *Clin Oncol.* (2009) 21:464–72. doi: 10.1016/j.clon.2009.04.007
- Giesel FL, Kratochwil C, Lindner T, Marschalek MM, Loktev A, Lehnert W, et al. 68Ga-FAPI PET/CT: biodistribution and preliminary dosimetry estimate of 2 DOTA-containing FAP-targeting agents in patients with various cancers. *J Nucl Med.* (2019) 60:386–92. doi: 10.2967/jnumed.118.215913
- Kratochwil C, Flechsig P, Lindner T, Abderrahim L, Altmann A, Mier W, et al. 68Ga-FAPI PET/CT: tracer uptake in 28 different kinds of cancer. *J Nuclear Med.* (2019) 60:801–5. doi: 10.2967/jnumed.119.227967
- Kelly T. Fibroblast activation protein-alpha and dipeptidyl peptidase IV (CD26): cell-surface proteases that activate cell signaling and are potential targets for cancer therapy. *Drug Resist Updat.* (2005) 8:51–8. doi: 10.1016/j.drug.2005.03.002
- Christiansen VJ, Jackson KW, Lee KN, McKee PA. Effect of fibroblast activation protein and α 2-antiplasmin cleaving enzyme on collagen Types I, III, and IV. *Arch Biochem Biophys.* (2007) 457:177–86. doi: 10.1016/j.abb.2006.11.006
- Henriksson ML, Edin S, Dahlin AM, Oldenborg P-A, Öberg Å, Van Guelpen B, et al. Colorectal cancer cells activate adjacent fibroblasts resulting in FGF1/FGFR3 signaling and increased invasion. *Am J Pathol.* (2011) 178:1387–94. doi: 10.1016/j.ajpath.2010.12.008
- Higashino N, Koma Y-I, Hosono M, Takase N, Okamoto M, Kodaira H, et al. Fibroblast activation protein-positive fibroblasts promote tumor progression through secretion of CCL2 and interleukin-6 in esophageal squamous cell carcinoma. *Lab Invest.* (2019) 99:777–92. doi: 10.1038/s41374-018-0185-6

22. Yang X, Lin Y, Shi Y, Li B, Liu W, Yin W, et al. FAP promotes immunosuppression by cancer-associated fibroblasts in the tumor microenvironment via STAT3–CCL2 signaling. *Cancer Res.* (2016) 76:4124–35. doi: 10.1158/0008-5472.CAN-15-2973
23. Chen L, Qiu X, Wang X, He J. FAP positive fibroblasts induce immune checkpoint blockade resistance in colorectal cancer via promoting immunosuppression. *Biochem Biophys Res Commun.* (2017) 487:8–14. doi: 10.1016/j.bbrc.2017.03.039
24. Xia Q, Geng F, Zhang F-F, Liu C-L, Xu P, Lu Z-Z, et al. Cyclophosphamide enhances anti-tumor effects of a fibroblast activation protein α -based DNA vaccine in tumor-bearing mice with murine breast carcinoma. *Immunopharmacol Immunotoxicol.* (2017) 39:37–44. doi: 10.1080/08923973.2016.1269337
25. Singh PP, Sharma PK, Krishnan G, Craig Lockhart A. Immune checkpoints and immunotherapy for colorectal cancer. *Gastroenterol Rep.* (2015) 3:289–97. doi: 10.1093/gastro/gov053
26. Mesker WE, Junggebur JMC, Szuhai K, de Heer P, Morreau H, Tanke HJ, et al. The carcinoma-stromal ratio of colon carcinoma is an independent factor for survival compared to lymph node status and tumor stage. *Cell Oncol.* (2007) 29:387–98. doi: 10.1155/2007/175276
27. Lugli A, Kirsch R, Ajioka Y, Bosman F, Cathomas G, Dawson H, et al. Recommendations for reporting tumor budding in colorectal cancer based on the International Tumor Budding Consensus Conference (ITBCC) 2016. *Mod Pathol.* (2017) 30:1299–311. doi: 10.1038/modpathol.2017.46
28. Kishore S, Piscuoglio S, Kovac MB, Gylling A, Wenzel F. 3'-UTR poly (T/U) tract deletions and altered expression of EWSR1 are a hallmark of mismatch repair-deficient cancers. *Cancer Res.* (2014) 74:224–34. doi: 10.1158/0008-5472.CAN-13-2100
29. Cancer Genome Atlas Network. Comprehensive molecular characterization of human colon and rectal cancer. *Nature.* (2012) 487:330–7. doi: 10.1038/nature11252
30. Colaprico A, Silva TC, Olsen C, Garofano L, Cava C, Garolini D, et al. TCGAAbiolinks: an R/bioconductor package for integrative analysis of TCGA data. *Nucleic Acids Res.* (2016) 44:e71. doi: 10.1093/nar/gkv1507
31. Uhlen M, Zhang C, Lee S, Sjostedt E, Fagerberg L, Bidkhorji G, et al. A pathology atlas of the human cancer transcriptome. *Science.* (2017) 357:eaan2507. doi: 10.1126/science.aan2507
32. Robinson MD, McCarthy DJ, Smyth GK. edgeR: a bioconductor package for differential expression analysis of digital gene expression data. *Bioinformatics.* (2010) 26:139–40. doi: 10.1093/bioinformatics/btp616
33. Robinson MD, Oshlack A. A scaling normalization method for differential expression analysis of RNA-seq data. *Genome Biol.* (2010) 11:R25. doi: 10.1186/gb-2010-11-3-r25
34. Yu G. clusterProfiler: An universal enrichment tool for functional and comparative study. *BioRxiv.* (2018) BioRxiv:256784. doi: 10.1101/256784
35. Sergushichev AA. An algorithm for fast preranked gene set enrichment analysis using cumulative statistic calculation. *BioRxiv.* (2016) BioRxiv:060012. doi: 10.1101/060012
36. Subramanian A, Tamayo P, Mootha VK, Mukherjee S, Ebert BL, Gillette MA, et al. Gene set enrichment analysis: a knowledge-based approach for interpreting genome-wide expression profiles. *Proc Natl Acad Sci USA.* (2005) 102:15545–50. doi: 10.1073/pnas.0506580102
37. Eide PW, Bruun J, Lothe RA, Sveen A. CMScaller: an R package for consensus molecular subtyping of colorectal cancer pre-clinical models. *Sci Rep.* (2017) 7:16618. doi: 10.1038/s41598-017-16747-x
38. Aran D, Hu Z, Butte AJ. xCell: digitally portraying the tissue cellular heterogeneity landscape. *Genome Biol.* (2017) 18:220. doi: 10.1186/s13059-017-1349-1
39. Hothorn T, Lausen B. On the exact distribution of maximally selected rank statistics. *Comput Statist Data Anal.* (2003) 43:121–37. doi: 10.1016/S0167-9473(02)00225-6
40. Guinney J, Dienstmann R, Wang X, de Reyniès A, Schlicker A, Soneson C, et al. The consensus molecular subtypes of colorectal cancer. *Nat Med.* (2015) 21:1350–6. doi: 10.1038/nm.3967
41. Santos AM, Jung J, Aziz N, Kissil JL, Puré E. Targeting fibroblast activation protein inhibits tumor stromagenesis growth in mice. *J Clin Invest.* (2009) 119:3613–25. doi: 10.1172/JCI38988
42. Lee H-O, Mullins SR, Franco-Barraza J, Valianou M, Cukierman E, Cheng JD. FAP-overexpressing fibroblasts produce an extracellular matrix that enhances invasive velocity and directionality of pancreatic cancer cells. *BMC Cancer.* (2011) 11:245. doi: 10.1186/1471-2407-11-245
43. Garin-Chesa P, Old LJ, Rettig WJ. Cell surface glycoprotein of reactive stromal fibroblasts as a potential antibody target in human epithelial cancers. *Proc Natl Acad Sci USA.* (1990) 87:7235–9. doi: 10.1073/pnas.87.18.7235
44. Huang Y. Sepsis promotes rapid tumor growth and increased microvessel density in a mouse model of human breast cancer. *Cancer Res.* (2004) 64:2712–6. doi: 10.1158/0008-5472.CAN-03-3184
45. Hartenbach EM, Olson TA, Goswitz JJ, Mohanraj D, Twigg LB, Carson LE, et al. Vascular endothelial growth factor (VEGF) expression and survival in human epithelial ovarian carcinomas. *Cancer Lett.* (1997) 121:169–75. doi: 10.1016/S0304-3835(97)00350-9
46. Joo HJ, Oh DK, Kim YS, Lee KB, Kim SJ. Increased expression of caveolin-1 and microvessel density correlates with metastasis and poor prognosis in clear cell renal cell carcinoma. *BJU Int.* (2004) 93:291–6. doi: 10.1111/j.1464-410X.2004.04604.x
47. Guetz GD, Des Guetz G, Uzzan B, Nicolas P, Cucherat M, Morere J-F, et al. Microvessel density and VEGF expression are prognostic factors in colorectal cancer. Meta-analysis of the literature. *Br J Cancer.* (2006) 94:1823–32. doi: 10.1038/sj.bjc.6603176
48. Cheng JD, Dunbrack RL, Valianou M, Rogatko A, Alpaugh RK, Weiner LM. Promotion of tumor growth by murine fibroblast activation protein, a serine protease, in an animal model. *Cancer Res.* (2002) 62:4767–72.
49. Koczorowska MM, Tholen S, Bucher F, Lutz L, Kizhakkedathu JN, De Wever O, et al. Fibroblast activation protein- α , a stromal cell surface protease, shapes key features of cancer associated fibroblasts through proteome and degradome alterations. *Mol Oncol.* (2016) 10:40–58. doi: 10.1016/j.molonc.2015.08.001
50. Le DT, Uram JN, Wang H, Bartlett B, Kemberling H, Eyring A, et al. PD-1 blockade in tumors with mismatch repair deficiency. *J Clin Oncol.* (2015) 33:LBA100. doi: 10.1200/jco.2015.33.18_suppl.lba100
51. Wikberg ML, Edin S, Lundberg IV, Van Guelpen B, Dahlin AM, Rutegård J, et al. High intratumoral expression of fibroblast activation protein (FAP) in colon cancer is associated with poorer patient prognosis. *Tumour Biol.* (2013) 34:1013–20. doi: 10.1007/s13277-012-0638-2
52. Son GM, Kwon M-S, Shin D-H, Shin N, Ryu D, Kang C-D. Comparisons of cancer-associated fibroblasts in the intratumoral stroma and invasive front in colorectal cancer. *Medicine.* (2019) 98:e15164. doi: 10.1097/MD.00000000000015164
53. Akagi Y, Adachi Y, Ohchi T, Kinugasa T, Shirouzu K. Prognostic impact of lymphatic invasion of colorectal cancer: a single-center analysis of 1,616 patients over 24 years. *Anticancer Res.* (2013) 33:2965–70.
54. Koelzer VH, Zlobec I, Lugli A. Tumor budding in colorectal cancer—ready for diagnostic practice? *Human Pathol.* (2016) 47:4–19. doi: 10.1016/j.humpath.2015.08.007
55. Wu Q-Q, Zhao M, Huang G-Z, Zheng Z-N, Chen Y, Zeng W-S, et al. Fibroblast activation protein (FAP) overexpression induces epithelial-mesenchymal transition (EMT) in oral squamous cell carcinoma by down-regulating dipeptidyl peptidase 9 (DPP9). *OncoTargets Therap.* (2020) 13:2599–611. doi: 10.2147/OTT.S243417
56. Sandberg TP, Maaik PM, Oosting J, Rob AE, Sier CFM, Mesker WE. Increased expression of cancer-associated fibroblast markers at the invasive front and its association with tumor-stroma ratio in colorectal cancer. *BMC Cancer.* (2019) 19:284. doi: 10.1186/s12885-019-5462-2
57. Park JE, Lenter MC, Zimmermann RN, Garin-Chesa P, Old LJ, Rettig WJ. Fibroblast activation protein, a dual specificity serine protease expressed in reactive human tumor stromal fibroblasts. *J Biol Chem.* (1999) 274:36505–12. doi: 10.1074/jbc.274.51.36505
58. Fearon DT. The carcinoma-associated fibroblast expressing fibroblast activation protein and escape from immune surveillance. *Cancer Immunol Res.* (2014) 2:187–93. doi: 10.1158/2326-6066.CIR-14-0002
59. Wen X, He X, Jiao F, Wang C, Sun Y, Ren X, et al. Fibroblast activation protein- α -positive fibroblasts promote gastric cancer progression and resistance to immune checkpoint blockade. *Oncol Res Featur Preclini Clin Cancer Therap.* (2017) 25:629–40. doi: 10.3727/096504016X14768383625385

60. Charo IF, Taubman MB. Chemokines in the pathogenesis of vascular disease. *Circul Res.* (2004) 95:858–66. doi: 10.1161/01.RES.0000146672.10582.17
61. Steiner JL, Angela Murphy E. Importance of chemokine (CC-motif) ligand 2 in breast cancer. *Int J Biol Mark.* (2012) 27:179–85. doi: 10.5301/JBM.2012.9345
62. Chun E, Lavoie S, Michaud M, Gallini CA, Kim J, Soucy G, et al. CCL2 promotes colorectal carcinogenesis by enhancing polymorphonuclear myeloid-derived suppressor cell population and function. *Cell Rep.* (2015) 12:244–57. doi: 10.1016/j.celrep.2015.06.024
63. Costa A, Kieffer Y, Scholer-Dahirel A, Pelon F, Bourachot B, Cardon M, et al. Fibroblast heterogeneity and immunosuppressive environment in human breast cancer. *Cancer Cell.* (2018) 33:463–79.e10. doi: 10.1016/j.ccell.2018.01.011

Conflict of Interest: The authors declare that the research was conducted in the absence of any commercial or financial relationships that could be construed as a potential conflict of interest.

Copyright © 2020 Coto-Llerena, Ercan, Kancherla, Taha-Mehlitz, Eppenberger-Castori, Soysal, Ng, Bolli, von Flüe, Nicolas, Terracciano, Fani and Piscuoglio. This is an open-access article distributed under the terms of the Creative Commons Attribution License (CC BY). The use, distribution or reproduction in other forums is permitted, provided the original author(s) and the copyright owner(s) are credited and that the original publication in this journal is cited, in accordance with accepted academic practice. No use, distribution or reproduction is permitted which does not comply with these terms.